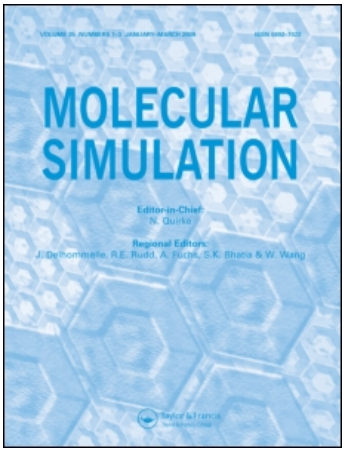

Molecular Simulation
Publication details, including instructions for authors and subscription information:
http://www.informaworld.com/smpp/title~content=t713644482

Molecular dynamics simulation of polyelectrolyte with oppositely charged monomeric and dimeric surfactants

Y. Xu[a]; J. Feng[b]; H. Liu[a]; Y. Hu[a]; J. Jiang[c]
[a] Lab for Advanced Materials and Department of Chemistry, East China University of Science and Technology, Shanghai, P. R. China [b] Department of Chemistry, Chuzhou University, Anhui, P. R. China [c] Department of Chemical & Biomolecular Engineering, National University of Singapore, Singapore

To cite this Article Xu, Y. , Feng, J. , Liu, H. , Hu, Y. and Jiang, J.(2007) 'Molecular dynamics simulation of polyelectrolyte with oppositely charged monomeric and dimeric surfactants', Molecular Simulation, 33: 3, 261 — 268
To link to this Article: DOI: 10.1080/08927020601158679
URL: http://dx.doi.org/10.1080/08927020601158679

Molecular Simulation, Vol. 33, No. 3, 15 March 2007, 261–268

Taylor & Francis
Taylor & Francis Group

Molecular dynamics simulation of polyelectrolyte with oppositely charged monomeric and dimeric surfactants

Y. XU†, J. FENG†‡, H. LIU†*, Y. HU† and J. JIANG¶

†Lab for Advanced Materials and Department of Chemistry, East China University of Science and Technology, Shanghai 200237, P. R. China
‡Department of Chemistry, Chuzhou University, Chuzhou, 239012 Anhui, P. R. China
¶Department of Chemical & Biomolecular Engineering, National University of Singapore, 4 Engineering Drive 4, Singapore 117576

(Received June 2006; in final form November 2006)

Interactions of anionic polyelectrolyte (PE) with cationic monomeric (MS) and dimeric surfactants (DS) have been investigated by coarse-grained molecular dynamics (MD) simulation. A PE/surfactant mixture is observed to evolve over time into micellar complex of increasing size. The critical aggregation concentration (CAC) is qualitatively found to be much lower than the critical micellization concentration (CMC) of the free surfactant. Compared to the monomeric analog, a DS interacts more strongly with the oppositely charged polyion chain. The equilibrium complex size becomes larger with increasing surfactant concentration. Simulation results are consistent with experimental observations and reveal that the electrostatic and hydrophobic interactions play an important role in the formation of micellar complex.

Keywords: Molecular dynamics; Polyelectrolyte; Surfactant; Interactions

1. Introduction

Polyelectrolyte (PE) and ionic surfactant mixtures have received considerable attention because of their unique properties and wide spectrum of industrial applications [1]. The strong electrostatic attraction between oppositely charged polyion chain and ionic head group in surfactant can lead to the formation of micellar complex at a critical aggregation concentration (CAC) [2], which is usually a few orders of magnitude lower than the critical micellization concentration (CMC), the concentration threshold for free surfactant to aggregate into micelles. The participation of PE in the aggregation significantly decreases the repulsion force between ionic head groups, consequently, PE induced micelles are more compact and stable [3].

Numerous experimental studies have been devoted to PE/surfactant mixtures [4–18]. In the structural analysis of sodium poly(styrenesulfonate) (NaPSS) and dodecyl- (DPC) and cetylpyridinium chlorides (CPC), Ksenija *et al.* [8] found that surfactant aggregated into spherical PE-induced micelles at various surfactant to polyelectrolyte (S/P) molar ratios, and the micelles grew in size with increasing S/P ratio. Guillot *et al.* [9,10] examined the interactions between anionic carboxymethylcellulose and cationic dodecyltrimethylammonium bromide (DTAB). Mixed surfactant/polymer aggregates were observed to form above a CAC of the surfactant accompanied by a rapid collapse of the polymer chains and the size of aggregate increased with increasing surfactant concentration.

Alternatively, theoretical approaches have been reported to investigate interactions between PE and surfactant [19–27]. Kuhn *et al.* [22–24] presented a mean-field theory for complex formation between a rigid PE and an ionic surfactant, which fairly well elucidated the experimentally observed cooperative transition of condensed counterions being replaced by surfactant. Diamant and Andelman [25,26] developed a chemical association theory to study the collapse of semi-flexible and flexible polymers due to the existence of small surfactant molecules, where the long-ranged electrostatic interactions were neglected. By means of a self-consistent field lattice model with a spherically symmetric frame, Wallin and Linse [27] predicted the formation of a micellar complex comprising a core of neutral surfactant tails along with a corona of surfactant heads and oppositely charged PE chains.

Molecular simulations have played an increasingly important role in disclosing the microscopic mechanism

*Corresponding author. Tel.: + 86-21-64252921. Email: hlliu@ecust.edu.cn

Molecular Simulation
ISSN 0892-7022 print/ISSN 1029-0435 online © 2007 Taylor & Francis
http://www.tandf.co.uk/journals
DOI: 10.1080/08927020601158679

of complex formation between PE and surfactant. This is the consequence of ever-growing computational resource and of the development in robust simulation algorithms. By using Monte Carlo (MC) simulations, Ferber and Löwen [28,29] established a "phase diagram" for a single PE chain with ionic surfactants based on the different strengths of long-range electrostatic and short-range hydrophobic interactions. Granfeldt *et al.* [30], Wallin and Linse [31–33] also employed MC simulations to assess the behavior of PE at charged micelles, in which an ionic surfactant molecule was simply represented by a large charged spherical particle. In addition, a recently developed mesoscopic simulation technique called dissipative particle dynamics (DPD) [34,35] has been applied to analyze the aggregation of PE and surfactant [36,37]. The salient feature in DPD is that relatively long time and length scales can be accessible [38,39].

The mixtures of PE and traditional ionic surfactant have been widely studied by a large number of experimental, theoretical and simulation studies, whereas the interactions between PE and gemini surfactant have not been fully understood. A gemini surfactant molecule is composed of two identical traditional monomeric surfactant (MS) molecules linked by a spacer chain, thus it is also called dimeric surfactant (DS). Widespread research on gemini surfactants has been stimulated by their superior properties to the traditional surfactants, e.g. increased surface activity, lower CMC and useful viscoelastic properties such as effective thickening [40]. Thus far the interactions between gemini surfactant and oppositely charged PE have been explored largely by experimental methods [41–50] and simulation studies are scarce. However, simulation can provide a detailed microscopic picture at a molecular level, which is otherwise experimentally difficult to characterize and therefore simulation can elucidate the underling physics. In this work, by using molecular dynamics (MD) simulation we investigate the interactions in two mixtures, one is MS/PE and the other is DE/PE. The long-ranged electrostatic and short-ranged hydrophobic interactions are explicitly accounted for in our MD simulations. Following a brief description of the models and methodology used, simulation results are presented. We first show how a surfactant/PE mixture evolves over time and then focus on how equilibrium structural properties, including polyion conformation, complex size and local structure, change with the increased concentration of surfactant. The differences between the two mixtures are compared and discussed.

2. Models and simulation method

A PE and surfactant mixed solution is described by a mesoscopic coarse-grained model. Solvent is treated as a continuous medium with a permittivity ξ. PE is represented by flexible linear polyion chain and corresponding counterion, in which a polyion chain has

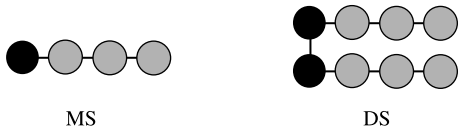

Figure 1. Schematic models of MS and DS. Counterions are not shown. • :head group; ◉ :tail group.

50 connected negatively charged particles. A MS molecule consists of one positively charged head particle connected to three neutral tail particles, while a DS molecule consists of two identical MS molecules with connection at the two heads. Figure 1 illustrates the schematic models for MS and DS, however, the counterions are not shown. For simplicity, all the particles in MS/PE and DS/PE mixtures are assumed to have the same mass m and diameter σ. Nevertheless, the extension to a general case is straightforward.

The short-range interaction between particles i and j at a distance r in the system is mimicked by the Lennard–Jones (LJ) potential,

$$u_{ij}^{\mathrm{LJ}}(r) = 4\varepsilon[(\sigma/r)^{12} - (\sigma/r)^{6}], \tag{1}$$

where ε is the well depth, r_c is the cutoff length. For the continuities of both potential energy and force at r_c, we adopt a truncated and shifted LJ potential, [51]

$$u'^{\mathrm{LJ}}_{ij}(r) = \begin{cases} 4\varepsilon[(\sigma/r)^{12} - (\sigma/r)^{6}] - u_c + f_c(r - r_c) & r \le r_c \\ 0 & r > r_c \end{cases}, \tag{2}$$

where u_c and f_c are the potential energy and force at r_c, respectively. From equation (1), we have

$$u_c = u_{ij}^{\mathrm{LJ}}(r_c) = 4\varepsilon[(\sigma/r_c)^{12} - (\sigma/r_c)^{6}], \tag{3}$$

$$f_c = -\mathrm{d}u_{ij}^{\mathrm{LJ}}(r)/\mathrm{d}r|_{r=r_c} = 24\varepsilon\sigma^6(1/r_c)^{13}(2\sigma^6 - r_c^6), \tag{4}$$

For particles of like charge $r_c = 2^{1/6}\sigma$, consequently, there is purely repulsive interaction; while for all other particles $r_c = 2.5\sigma$.

The long-range interaction between charged particles i and j with charges z_i and z_j is mimicked by the Coulombic potential,

$$u_{ij}^{\mathrm{ELE}}(r) = \frac{e^2}{4\pi\xi}\frac{z_i z_j}{r}, \tag{5}$$

where e is unit charge.

The connective interaction of two bonded particles within polyion chain or surfactant is modeled by a finite extension nonlinear elastic potential (FENE),

$$u_{ij}^{\mathrm{FENE}}(r) = \begin{cases} -\frac{1}{2}kR_0^2\ln\left(1 - r^2/R_0^2\right) & r \le R_0 \\ 0 & r > R_0 \end{cases}, \tag{6}$$

where $k = 18\varepsilon/\sigma^2$ is the spring constant, and $R_0 = 2\sigma$ is the maximum extension. With these parameters, the average fluctuation of bond length was found to be about 5%.

The coarse-grained model adopted here for PE and surfactant do not account for the molecular details, however, they capture the essential characteristics of realistic PE and surfactant in terms of long-range electrostatic interaction, short-range dispersive interaction, chain connectivity, excluded volume and internal flexibility.

The motion of each particle in the system is governed by the stochastic Langevin equation, which accounts for the viscous force from solvent and the stochastic force from heat-bath, [52,53]

$$m\ddot{\mathbf{r}}_i = -\nabla U_i - \gamma \dot{\mathbf{r}}_i + \mathbf{W}_i(t), \tag{7}$$

where $\mathbf{r}_i$ is the position of particle i, γ is a friction coefficient set equal to 1 in this work. $\mathbf{W}_i(t)$ is a random force exerting on particle i at time t, which satisfies

$$\langle \mathbf{W}_i(t)\mathbf{W}_i(t')\rangle = 6k_{\mathrm{B}}T\gamma\delta_{ij}\delta(t-t'), \tag{8}$$

U_i is the interaction energy of particle i with all the other particles

$$U_i = \sum_{j\neq i} u_{ij}(r) = \sum_{j\neq i}\left[u_{ij}^{\mathrm{ELE}}(r) + u_{ij}^{\mathrm{LJ}}(r) + u_{ij}^{\mathrm{FENE}}(r)\right] \tag{9}$$

In our MD simulations, a cubic box with a length $L = 100\sigma$ was used with the periodic boundary conditions in all three dimensions. The simulation box was found to be sufficiently large to eliminate the finite size effect. Each system in simulation contained five PE molecules and various numbers of MS or DS molecules. The temperature under consideration was $k_{\mathrm{B}}T/\varepsilon = 1$, where k_{B} is the Boltzmann constant, T is the absolute temperature of system and the Bjerrum length $e^2/(4\pi\xi k_{\mathrm{B}}T)$ was set equal to σ. It implies that each particle in our simulation has a diameter $\sigma = 7.145$ Å in an aqueous solution at 298.15 K. Surface-force measurements reveal that the size of a sodium dodecyl sulfate micelle is approximately 40 Å [54], which is substantially larger than individual particle.

Ewald summation method was used to calculate the electrostatic energy, which was decomposed into the real space contribution and the reciprocal space contribution [55,56]. The half box length was selected as the cutoff distance in the real space and the real/reciprocal space partition parameter in the error function was chosen to be $5/L$. The number of reciprocal lattice vectors was chosen automatically by the code in such a way that the relative deviation of electrostatic energy was less than 0.01%. The virial of electrostatic contribution was set equal to the negative of the electrostatic potential. The initial bond lengths for polyions and surfactants were all set equal to σ. The integral time step is 0.005τ, where $\tau = \sigma(m/\varepsilon)^{1/2}$. The total time steps of simulation evolution were 2×10^6, in which the last 2×10^5 steps were used to obtain ensemble averages.

3. Results and discussion

3.1 Time evolution

Figure 2 shows the dynamic snapshots of a DS/PE mixture with $n = 12$ at different times, in which n is the number of surfactant head groups with respect to the number of polyion chains. Note that counterions of PE and DS are not shown in the figure. Five PE molecules exist in this mixture, consequently, there are $12\times5 = 60$ DS head groups. At $t = 0$, all the five polyions are in a relatively stretched conformation with only a few DS molecules adsorbed discretely along each polyion. At $t = 2500\tau$ and 5000τ, more than two polyion chains are partially bound by several DS molecules to form complex and show random coiled structures. At $t = 7500\tau$ and $10{,}000\tau$, almost all the five polyions are bound with appreciable number of DS molecules to form nearly spherical compact complex and there are some free DS molecules existing in the mixture. While figure 2 shows the time evolution of a DS/PE mixture with a given n, we show below the effect of n on equilibrium structural properties in both MS/PE and DS/PE mixtures.

3.2 Polyion conformation

Polyion conformation can be quantitatively characterized by the radius of gyration R_{g} and the end-to-end distance R_{e}. Shown in figure 3 are the root-mean-squared R_{g} and R_{e} of polyion as a function of n in MS/PE and DS/PE mixtures. With increasing n, both R_{g} and R_{e} in either mixture exhibit similar trends. In the absence of surfactant ($n = 0$), polyion is primarily stretched as shown in figure 4(a) because of the electrostatic repulsion between the monomers of like charges, thus both R_{g} and R_{e} have the maximal values. With the addition of surfactant, R_{g} and R_{e} drop rapidly, in other words, polyion collapses. This is due to the strong electrostatic attraction of polyion with surfactant ionic head groups and sequent binding of surfactant molecules onto polyion chain, as shown in figure 4(b) and (d) at $n = 12$. As a result, the electrostatic repulsion between polyion monomers is substantially screened; polyion chain shows random coiled conformation. During this process, the counterions in the vicinity of polyion are replaced by surfactants. The R_{g} and R_{e} continue to decrease until $n = 40$ and then level off with small fluctuations. Nevertheless, as we will see that the complex size continues growing.

At a given n, i.e. the concentration of DS is half that of MS, R_{g} and R_{e} in a DS/PE mixture are consistently smaller compared to a MS/PE mixture. This is because a DS molecule has two ionic head groups and has a stronger electric field than a MS molecule; it thus interacts more strongly with oppositely charged polyion chain. This has been observed in our recent experimental studies for the interactions of sodium polyacrylate separately with hexylene-1,6-bis(dodecyldimethylammonium bromide) and DTAB, [44,57] and of bovine serum albumin with alkanediyl-α,ω-bis(dimethyldodecyl-ammonium

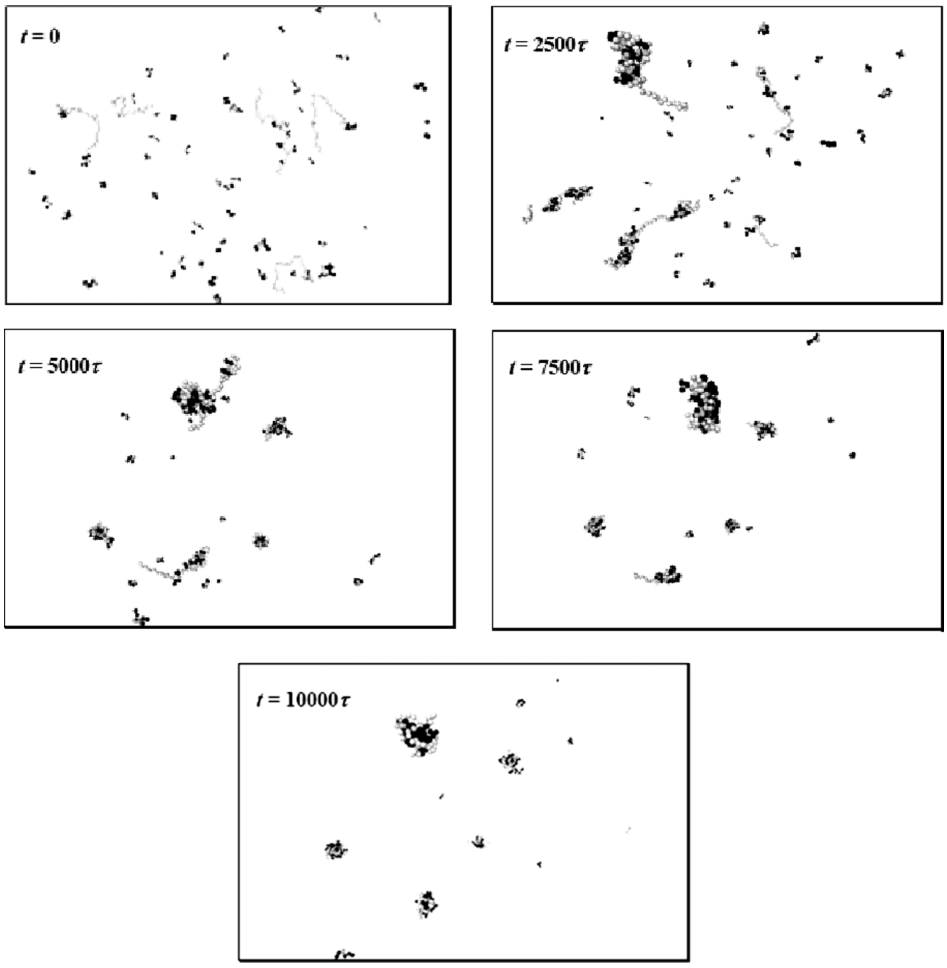

Figure 2. Time evolution of a DS/PE mixture with $n = 12$ (counterions of PE and surfactants are not shown).

bromide) and DTAB [58]. Consequently, more DS molecules are bound onto polyion chain, which leads to a stronger electrostatic shielding effect and a more compact complex.

From figure 3, we can see that the aggregation of MS or DS onto polyion begins at a very low surfactant concentration. No free micelle is found to form by surfactant itself at the highest $n = 160$ considered in our simulations. Our additional simulations of free surfactant in box of same size show that free micelle starts to appear when the number of surfactant molecules reach 140 and 60 in MS and DS, respectively, which could be regarded as a rough estimation of the CMC. This is, the corresponding ratio n are 28 and 24 in MS/PE and DS/PE mixtures, respectively. Qualitatively, the CAC in either mixture is far below the CMC. PE facilitates the oppositely charged ionic surfactants to aggregate by suppressing the electrostatic repulsion between ionic head groups. Such behavior is well recognized and has been observed in experimental studies. Quantitatively, we can estimate the

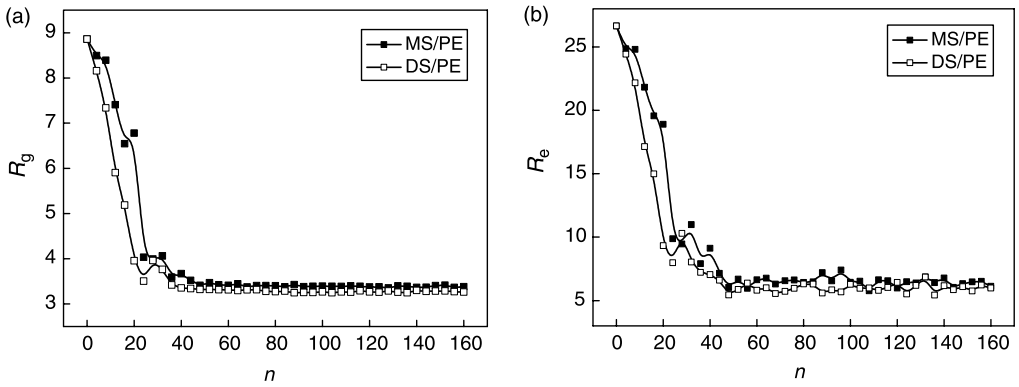

Figure 3. Root-mean-squared (a) radius of gyration R_g and (b) end-to-end distance R_e of polyion as a function of n in MS/PE ad DS/PE mixtures.

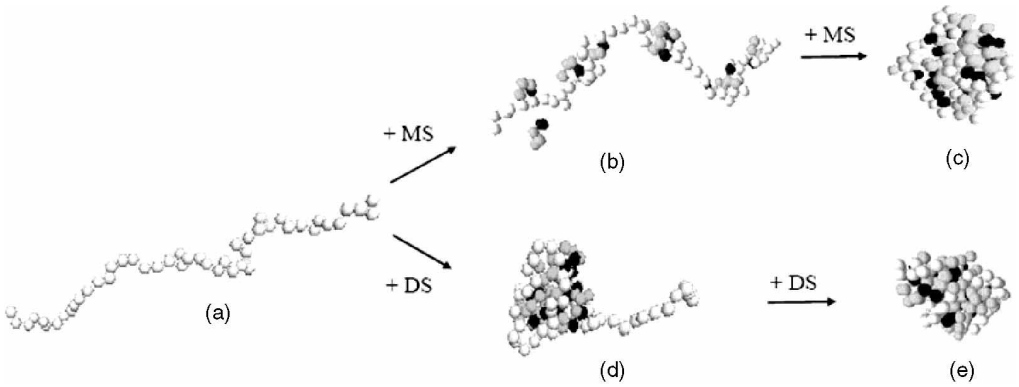

Figure 4. Equilibrium snapshots at different n in MS/PE ad DS/PE mixtures (counterions of PE and surfactants are not shown). (a) $n = 0$; (b) and (d) $n = 12$; (c) and (e) $n = 40$. ○ :polyion monomer; • :head group of surfactant; ◍ :tail group of surfactant.

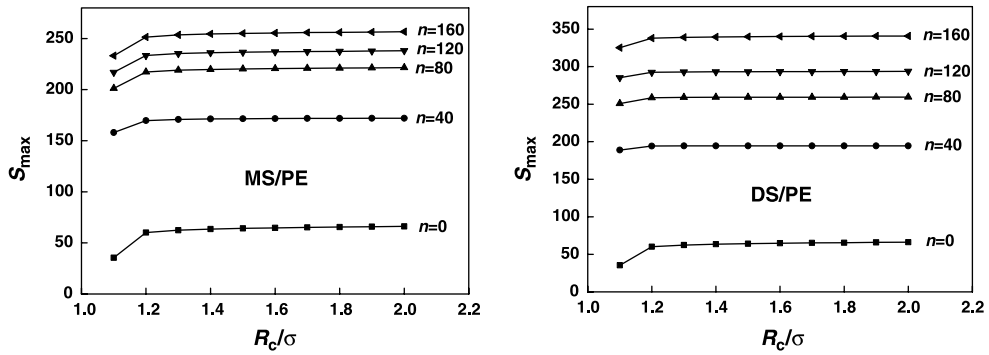

Figure 5. Ensemble averaged maximal complex size S_{max} as a function of cutoff distance R_c at various n in MS/PE and DS/PE mixtures.

value of CMC by removing the polyion and seeing at what concentration micellar formation starts to take place, just as aforementioned. However, this time-consuming method is not accurate and cannot be easily implemented to predict the value of CAC. Therefore, a more effective technique for quantitative predictions of the CMC and CAC is yet to be developed.

3.3 Complex size

The changes of R_g and R_e with n in figure 3 indicate that further addition of surfactant beyond $n = 40$ has little influence on the change of polyion conformation. However, the micellar complex still increases in size with increasing surfactant concentration. This suggests that there is no unique relation between polyion conformation and complex formation. In our simulations, all the particles were assumed to have an identical size; the complex size was quantified by the number of particles constituting an aggregate. If the distance between one of the particles in an aggregate and that in another aggregate is within a given cutoff R_c, the two aggregates are considered to be one. Consequently, the size is expected to depend on the value of R_c, as shown in figure 5. At a given n, the ensemble averaged maximal complex size S_{max} first increases with increasing R_c in either MS/PE or DS/PE mixture and then approaches a constant value beyond $R_c \approx 1.6\sigma$.

Figure 6 shows the maximal complex size S_{max} as a function of n at $R_c = 1.6\sigma$. In general, the complex size becomes bigger as the surfactant concentration increases, as observed in many experimental studies [8–10,42–44]. The behavior of S_{max} can be divided into two regions at $n = 40$. In AB/DE region, while there is a steep drop in R_g and R_e, S_{max} increases rapidly. This is due to the strong electrostatic attraction between polyions and surfactant head groups. In BC/EF region, R_g and R_e hardly change, whereas S_{max} increases slowly and tends to reach a constant. In this region, the binding sites on polyions have reached saturation and further added surfactants cannot

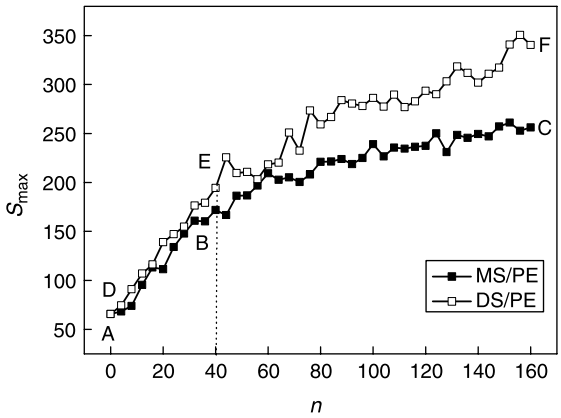

Figure 6. Ensemble averaged maximal complex size S_{max} as a function of n at $R_c = 1.6\sigma$ in MS/PE and DS/PE mixtures.

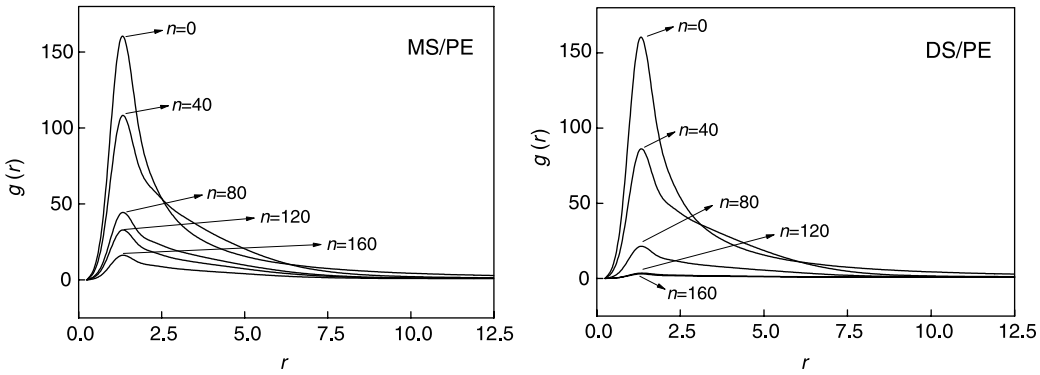

Figure 7. Radial distribution function $g(r)$ between the polyion monomer and its counterion at different n in MS/PE and DS/PE mixtures.

form new micellar complex, but rather enter into the existing complex through the hydrophobic attraction between tail groups. Compared to the electrostatic attraction, the hydrophobic attraction is weaker; consequently, the increase in size in the second region is slower than the first region. At a given n, the maximal complex size in DS/PE is consistently larger than that in MS/PE. This is because of the chemical connection between the two ionic heads in DS, which leads DS to form aggregate more easily and a stronger interaction between DS and PE.

3.4 Local structure

The local structure is characterized by the radial distribution function $g(r)$. Figure 7 shows $g(r)$ between the polyion monomer and its counterion at various n in MS/PE and DS/PE mixtures, respectively. In the absence of surfactant, some of counterions are in the close vicinity of polyion due to the electrostatic attraction. Upon addition of surfactant, however, complex starts to form gradually between polyion and surfactant and counterions are replaced by surfactants and released. As a result, $g(r)$ peak intensity becomes smaller. The higher the surfactant concentration is, the more significant this effect is. Furthermore, this effect is more distinct in DS/PE mixture, in which $g(r)$ peak is smaller than that in MS/PE mixture at a given n.

Figure 8 shows $g(r)$ between the polyion monomer and its counterion, head and tail groups of surfactant at a low ($n = 12$) and a high ($n = 120$) surfactant concentration in MS/PE and DS/PE mixtures, respectively. At $n = 12$, the local surfactant concentration near polyion chain is higher than the counterion concentration, particularly, the head group of the surfactant. This behavior is also observed at $n = 120$. This can be ascribed to the cooperative contributions of the electrostatic and hydrophobic interactions, of which the former plays a dominant role in the formation of surfactant/polyion complex. Upon comparison with MS/PE mixture, $g(r)$ peaks in DS/PE mixture are significantly higher, showing that more DS molecules take part in complex formation and DS is more favorable to form complex with PE. Additionally, we have made some elementary studies on the influence of the spacer length of a gemini surfactant on its association behavior with PE. It can be found similarly through the radial distribution function in figure 9 that by increasing the length of the spacer, gemini surfactant has a weaker interaction with PE, for a longer spacer can make the two ionic head groups more separated leading to a weaker electric field.

4. Conclusions

By using MD simulation, we have examined the interactions in mixtures of anionic PE separately with cationic MS and DE. Strong electrostatic and hydrophobic attractions lead to the formation of micellar complex. With addition of surfactant, evidenced by the behavior in radius of gyration and end-to-end distance, the

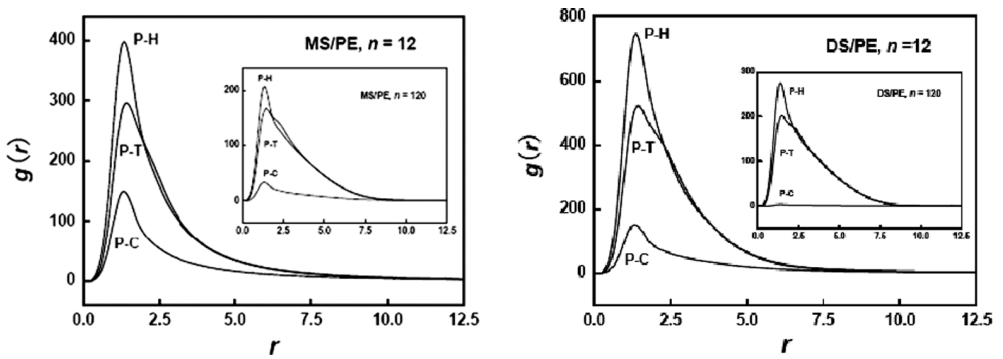

Figure 8. Radial distribution function $g(r)$ in MS/PE and DS/PE mixtures at $n = 12$. The inset is at $n = 120$. P, polyion monomer; H, head group of surfactant; T, tail group of surfactant; C, counterion of PE.

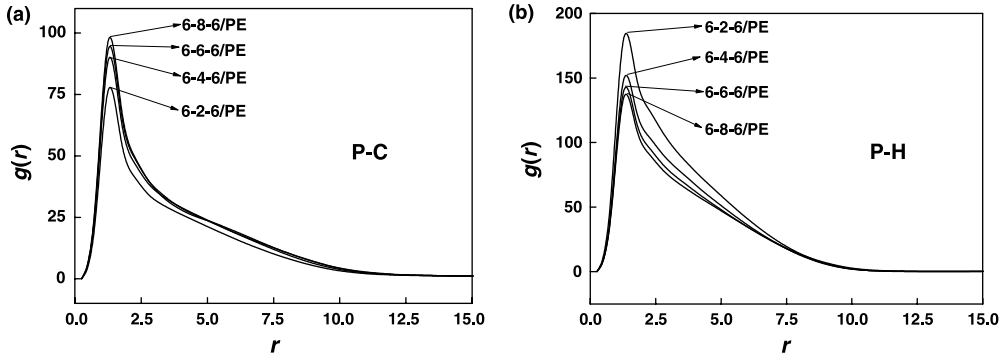

Figure 9. Radial distribution function $g(r)$ of polyion monomer (P) separately with its counterion (C) (a) and surfactant head (H) (b) at $n = 40$ in the mixture of PE with gemini surfactants of varying spacer chain lengths. The inside symbol *m-s-m* denotes a gemini surfactant composed of one spacer with *s* segments and two tails with *m* segments.

conformation of polyion chain changes from stretched to random coiled and to spherical and moreover, the micellar complex is observed to increase in size. The CAC of a surfactant/PE system is lower than the CMC of a free surfactant system; and a DS interacts more strongly with oppositely charged polyion chain than its monomeric analog. The simulation results in this work are consistent with experimental studies and provide microscopic insight into the aggregation process in PE and surfactant mixtures.

Acknowledgements

This work is supported by the National Natural Science Foundation of China (Projects No. 20236010, 20476025), the Doctoral Research Foundation sponsored by the Ministry of Education of China (Project No.20050251004), E-institute of Shanghai High Institution Grid (No.200303), and the National University of Singapore.

References

[1] A. Markus, B. Christian, T. Andreas. Polyelectrolyte–surfactant complexes: a new class of highly ordered polymer materials. *Trends Polym. Sci.*, **5**, 262 (1997).
[2] P. Hansson, B. Lindman. Surfactant–polymer interactions. *Curr. Opin. Colloid Interface Sci.*, **1**, 604 (1996).
[3] K. Kogej, J. Skerjanc. Fluorescence and conductivity studies of polyelectrolyte-induced aggregation of alkyltrimethylammonium bromides. *Langmuir*, **15**, 4251 (1999).
[4] P.S. Leung, E.D. Goddard, C. Han, C.J. Glinka. A study of polycation–anionic-surfactant systems. *Colloids Surf.*, **13**, 47 (1985).
[5] P.M. Macdonald, Y. Yue. Influence of polyelectrolytes on the surface electrostatics of charged colloids as determined using deuterium NMR. *Langmuir*, **9**, 1206 (1993).
[6] A. Hersloef, L.O. Sundeloef, K. Edsman. Interaction between polyelectrolyte and surfactant of opposite charge: hydrodynamic effects in the sodium hyaluronate/tetradecyl-trimethylammonium bromide/sodium chloride/water system. *J. Phys. Chem.*, **96**, 2345 (1992).
[7] P.M. Claesson, M. Bergstrom, A. Dedinaite, M. Kjellin, J.F. Legrand, I. Grillo. Mixtures of cationic polyelectrolyte and anionic surfactant studied with small-angle neutron scattering. *J. Phys. Chem. B*, **104**, 11689 (2000).
[8] K. Ksenija, T. Elisabeth, R. Harry. Formation of organized structures in systems containing alkylpyridinium surfactants and sodium poly(styrenesulfonate). *Acta Chim. Sloven.*, **48**, 353 (2001).
[9] S. Guillot, M. Delsanti, S. Desert, D. Langevin. Surfactant-induced collapse of polymer chains and monodisperse growth of aggregates near the precipitation boundary in carboxymethylcellulose-DTAB aqueous solutions. *Langmuir*, **19**, 230 (2003).
[10] S. Guillot, D. McLoughlin, N. Jain, M. Delsanti, D. Langevin. Polyelectrolyte–surfactant complexes at interfaces and in bulk. *J. Phys. Condens. Matter*, **15**, S219 (2003).
[11] K. Hayakawa, P.J. Santerre, J.C.T. Kwak. Study of surfactant–polyelectrolyte interactions. Binding of dodecyl- and tetradecyltrimethylammonium bromide by some carboxylic polyelectrolytes. *Macromolecules*, **16**, 1642 (1983).
[12] P.S. Leung, E.D. Goddard. Gels from dilute polymer/surfactant solutions. *Langmuir*, **7**, 608 (1991).
[13] I.S. Chronakis, P. Alexandridis. Rheological properties of oppositely charged polyelectrolyte–surfactant mixtures: effect of polymer molecular weight and surfactant architecture. *Macromolecules*, **34**, 5005 (2001).
[14] K. Hayakawa, J. Ohta, T. Maeda. Spectroscopic studies of dye solubilizates in micellelike complexes of surfactant with polyelectrolyte. *Langmuir*, **3**, 377 (1987).
[15] Y. Morishima, M. Mizusaki, K. Yoshida, P.L. Dubin. Interactions of micelles with fluorescence-labeled polyelectrolytes. *Colloids Surf. A*, **147**, 149 (1999).
[16] P. Chandar, P. Somasundaran, N.J. Turro. Fluorescence probe investigation of anionic polymer–cationic surfactant interactions. *Macromolecules*, **21**, 950 (1988).
[17] M. Almgren, P. Hansson, E. Mukhtar, J.V. Stam. Aggregation of alkyltrimethylammonium surfactants in aqueous poly(styrenesulfonate). *Langmuir*, **8**, 2405 (1992).
[18] I. Balomenou, G. Bokias. Water-soluble complexes between cationic surfactants and comb-type copolymers consisting of an anionic backbone and hydrophilic nonionic poly(*N*,*N*-dimethylacrylamide) side chains. *Langmuir*, **21**, 9038 (2005).
[19] K. Shirahama, H. Yuasa, S. Sugimoto. Binding of sodium decyl sulfate to a cationic polymer. *Bull. Chem. Soc. Jpn.*, **54**, 375 (1981).
[20] K. Shirahama, M. Tashiro. Binding of 1-decylpyridinium bromide to poly(vinyl sulfate). *Bull. Chem. Soc. Jpn.*, **57**, 377 (1984).
[21] R.P. Sear. Theory for polymer coils with necklaces of micelles. *J. Phys. Condens. Matter*, **10**, 1677 (1998).
[22] P.S. Kuhn, Y. Levin, M.C. Barbosa. Complex formation between polyelectrolytes and ionic surfactants. *Chem. Phys. Lett.*, **298**, 51 (1998).
[23] P.S. Kuhn, M.C. Barbosa, Y. Levin. Effects of hydrophobicity in DNA surfactant complexation. *Physica A*, **283**, 113 (2000).
[24] M.B.A. Silva, P.S. Kuhn, L.S. Lucena. DNA solutions with multivalent salts and amphiphiles. *Physica A*, **296**, 31 (2001).
[25] H. Diamant, D. Andelman. Binding of molecules to DNA and other semiflexible polymers. *Phys. Rev. E*, **61**, 6740 (2000).
[26] H. Diamant, D. Andelman. Self-assembly in mixtures of polymers and small associating molecules. *Macromolecules*, **33**, 8050 (2000).
[27] T. Wallin, P. Linse. Polyelectrolyte-induced micellization of charged surfactants. Calculations based on a self-consistent field lattice model. *Langmuir*, **14**, 2940 (1998).
[28] C. von Ferber, H. Löwen. Complexes of polyelectrolytes and oppositely charged ionic surfactants. *J. Chem. Phys.*, **118**, 10774 (2003).

[29] C. von Ferber, H. Löwen. Polyelectrolyte–surfactant complex: phases of self-assembled structures. *Faraday Discuss.*, **128**, 389 (2005).
[30] M.K. Granfeldt, Bo. Jönsson, C.E. Woodward. A Monte Carlo simulation study of the interaction between charged colloids carrying adsorbed polyelectrolytes. *J. Phys. Chem.*, **95**, 4819 (1991).
[31] T. Wallin, P. Linse. Monte Carlo simulations of polyelectrolytes at charged micelles 1. Effects of chain flexibility. *Langmuir*, **12**, 305 (1996).
[32] T. Wallin, P. Linse. Monte Carlo simulations of polyelectrolytes at charged micelles 2. Effects of linear charge density. *J. Phys. Chem.*, **100**, 17873 (1996).
[33] T. Wallin, P. Linse. Monte Carlo simulations of polyelectrolytes at charged micelles 3. Effects of surfactant tail length. *J. Phys. Chem. B*, **101**, 5506 (1997).
[34] P.J. Hoogerbrugge, J.M.V.A. Koelman. Simulating microscopic hydrodynamic phenomena with dissipative particle dynamics. *Europhys. Lett.*, **19**, 155 (1992).
[35] J.M.V.A. Koelman, P.J. Hoogerbrugge. Dynamic simulations of hard-sphere suspensions under steady shear. *Europhys. Lett.*, **21**, 363 (1993).
[36] R.D. Groot. Mesoscopic simulation of polymer–surfactant aggregation. *Langmuir*, **16**, 7493 (2000).
[37] R.D. Groot. Electrostatic interactions in dissipative particle dynamics(simulation of polyelectrolytes and anionic surfactants. *J. Chem. Phys.*, **118**, 11265 (2003).
[38] R.D. Groot, P.B. Warren. Dissipative particle dynamics: bridging the gap between atomistic and mesoscopic simulation. *J. Chem. Phys.*, **107**, 4423 (1997).
[39] R.D. Groot, T.J. Madden. Dynamic simulation of diblock copolymer microphase separation. *J. Chem. Phys.*, **108**, 8713 (1998).
[40] F.M. Menger, J.S. Keiper. Gemini surfactants. *Angew. Chem. Int. Ed.*, **39**, 1906 (2000).
[41] M. Pisárčik, M. Soldan, D. Bakos, F. Devínsky, I. Lacko. Viscometric study of the sodium hyaluronate-sodium chloride-alkyl-(*n*)-ammonium surfactant system. *Colloids Surf. A*, **150**, 207 (1999).
[42] M. Pisárčik, T. Imae, F. Devínsky, I. Lacko, F. Bakoš. Aggregation properties of sodium hyaluronate with alkanediyl-α,ω-bis(dimethyl-alkylammonium bromide) surfactants in aqueous sodium chloride solution. *J. Colloids Interface Sci.*, **228**, 207 (2000).
[43] M. Pisárčik, T. Imae, F. Devínsky, I. Lacko. Aggregates of sodium hyaluronate with cationic and aminoxide surfactants in aqueous solution—light scattering study. *Colloids Surf. A*, **183–185**, 555 (2001).
[44] Y.Y. Pi, Y.Z. Shang, C.J. Peng, H.L. Liu. Microstructure and phase behavior of cationic gemini/anionic polyelectrolyte/water ternary System. *Chinese J. Process Eng.*, **6**, 54 (2006).
[45] X.Y. Wang, J.B. Wang, Y.L. Wang, H.K. Yan. Salt effect on the complex formation between cationic gemini surfactant and anionic polyelectrolyte in aqueous solution. *Langmuir*, **20**, 9014 (2004).
[46] Y. Tomokazu, N. Yukiko, E. Kunio. Interactions of quaternary ammonium salt-type gemini surfactants with sodium poly(styrene sulfonate). *J. Colloid Interface Sci.*, **275**, 618 (2004).
[47] R. Zana, M. Benrraou. Interactions between polyanions and cationic surfactants with two unequal alkyl chains or of the dimeric type. *J. Colloid Interface Sci.*, **226**, 286 (2000).
[48] L. Karlsson, M.C.P. van Eijk, O. Söderman. Compaction of DNA by gemini surfactants: effects of surfactant architecture. *J. Colloids Interface Sci.*, **252**, 290 (2002).
[49] D. Ukríková, G. Rapp, P. Balgavý. Condensed lamellar phase in ternary DNA–DLPC-cationic gemini surfactant system: a small-angle synchrotron X-ray diffraction study. *Bioelectrochemistry*, **58**, 87 (2002).
[50] D. Ukríková, I. Zajac, M. Dubničková, M. Pisárčik, S.S. Funari, G. Rapp, P. Balgavý. Interaction of gemini surfactants butane-1,4-diyl-bis(alkyldimethylammonium bromide) with DNA. *Colloids Surf. B*, **42**, 59 (2005).
[51] R.L. Andrew. *Molecular Modeling, Principles and Applications*, Addison Wesley Longman Limited, (1996).
[52] G.S. Grest, K. Kremer. Molecular dynamics simulation for polymers in the presence of a heat bath. *Phys. Rev. A*, **33**, 3628 (1986).
[53] M.J. Stevens, K. Kremer. The nature of flexible linear polyelectrolytes in salt free solution: a molecular dynamics study. *J. Chem. Phys.*, **103**, 1669 (1995).
[54] P.M. Claesson, M.L. Fielden, A. Dedinaite, J. Brown. Interactions between a 30% charged polyelectrolyte and an anionic surfactant in bulk and at a solid–liquid interface. *J. Phys. Chem. B*, **102**, 1270 (1998).
[55] M.P. Allen, D.J. Tildesley. *Computer Simulation of Liquids*, p. 155, Clarendon, Oxford (1987).
[56] U. Essmann, L. Perera, M.L. Berkowitz. A smooth particle mesh ewald method. *J. Chem. Phys.*, **103**, 8577 (1995).
[57] Y.Y. Pi, Y.Z. Shang, C.J. Peng, H.L. Liu, Y. Hu, J.W. Jiang. Phase behavior of gemini surfactant hexylene-1,6-bis (dodecyldimethyl-ammonium bromide) and polyelectrolyte NaPAA. *J. Colloids Interface Sci.*, **299**, 410 (2006).
[58] Y.Y. Pi, Y.Z. Shang, C.J. Peng, H.L. Liu, Y. Hu, J.W. Jiang. Interactions between bovine serum albumin and gemini surfactant alkanediyl-α,ω-bis(dimethyldodecyl-ammonium bromide). *Biopolymers*, **83**, 243 (2006).